



# MPC-based Voltage Control with Reactive Power from High-Power Charging Stations for EVs

Jonatan Ralf Axel Klemets   
Dept. of Energy Systems  
SINTEF Energy Research  
Trondheim, Norway  
jonatan.klemets@sintef.no

Bendik Nybakk Torsæter   
Dept. of Energy Systems  
SINTEF Energy Research  
Trondheim, Norway  
bendik.torsater@sintef.no

**Abstract**—The recent development of EVs with high-capacity batteries and high charging power capabilities leads to an increased demand for fast-charging stations (FCS). However, FCS can cause power quality issues such as voltage drops in distribution grids with limited power capacity. Grid reinforcements are a standard solution for solving power quality issues. However, these can be costly. An alternative approach is to install bi-directional chargers at FCS and use this flexibility source to provide voltage support in peak-load periods by injecting reactive power to the grid. This paper proposes a model predictive controller (MPC) to control and coordinate such high-power chargers. The MPC maximizes the charging rate for the EVs while ensuring that the voltage level stays within the allowable limits. The control system has been evaluated through simulations on a realistic grid model, and the results show that both the FCS and the grid can benefit from utilizing the reactive power.

**Index Terms**—Model predictive control (MPC), Fast charging station (FCS), Electric vehicle (EV), Reactive power, Voltage control.

## I. INTRODUCTION

The concern of a limited range and long charging time prohibits consumers to fully embrace electric vehicles (EVs), where the term EV in this paper denotes electric cars. Therefore, the availability of fast-charging stations (FCS) is likely to be essential to increase the adoption of EVs in the future [1, 2]. However, the additional peak load from high-power charging at FCS can pose challenges for the existing distribution grid.

The grid impact from chargers with a slower charging rate, located at parking lots or in residential areas, have been investigated in [3] and [4]. In [3], a coordinating charging approach was proposed to improve the power quality and voltage deviations. Similarly, optimal scheduling algorithms based on model predictive control (MPC) have been developed in [5, 6]. These control systems are expecting the EVs to charge at long time intervals, and thus, they mainly focus on optimal scheduling and load-shifting.

For FCS, the problem is different since the aim is to provide high power for the short duration an EV is connected to

The authors would like to thank the Research Council of Norway and industry partners for the support in writing this paper under project 295133/E20 **FuChar - Grid and Charging Infrastructure of the Future**.

the charger. Today's chargers can charge up to 350 kW [7], and therefore, increased penetration of EVs with very high power requirements will impose significant demands on the grid. The aggregated load from FCS can also have a high peak-to-average power ratio, which implies a low utilization of the available grid capacity [8]. In addition, fast charging can often occur during peak hours when the load demands are high, making load-shifting very challenging. One solution is to include some additional energy storage systems (ESS) as a supply source during the peak-hours as in [1, 9].

Modern chargers can be equipped with bi-directional converters so that charging can take place in any of the four  $P-Q$  quadrants, thus, allowing active and reactive power flow in both directions. The concept of supplying active power to the grid from the batteries of connected EVs, is referred to as Vehicle-to-Grid (V2G). This allows EVs to provide ancillary services to the grid by temporarily discharging an EV's battery. A review of current V2G technologies and their impact on the distribution grid are available in [10] and [11].

The economic benefit from V2G services is still an open question, especially when accounting for battery degradation [12, 13]. Nevertheless, for FCS, the objective is to maximize the state of charge (SoC) for the short time the EV is charging. Therefore, services that involve discharging an EV's battery to compensate for slow voltage and frequency variations may be of little benefit, even though it could be useful for handling fast and short-term events [14]. However, when bi-directional converters are used, it is possible to inject reactive power into the grid while simultaneously consuming active power [15]. Voltage drops are one of the main issues caused by charging EVs [16], and thus, the charging capacity available for FCS can be restricted by the grid operators. However, for medium-voltage (MV) grids with a low R/X ratio, reactive power can contribute to voltage control [17]. Therefore, having the FCS inject reactive power while simultaneously consuming active power can benefit both the grid and FCS operators by reducing charging restrictions without needing to reinforce the grid [18].

In this work, an MPC is designed to control and coordinate the chargers at an FCS. The MPC tries to supply the charging EVs with the maximum amount of energy while keeping the voltages within allowable limits. When the voltage drops below the threshold, the MPC will initially inject reactive power

to the grid. If reactive power alone is not sufficient to satisfy the voltage constraints, the MPC will also restrict the active power delivered to the EVs. Previous research on MPC and EV charging has primarily been focusing on controlling active power for optimal scheduling and load shifting. However, little work has been done to utilize the reactive power available at an FCS. Therefore, the aim is to showcase the advantages of controlling both active and reactive power at an FCS.

## II. METHOD

An MPC is proposed to control and coordinate the chargers at an FCS. Implementing an MPC requires formulating an objective function, defining constraints, and developing dynamic models, which will be presented in this section.

### A. Model predictive control

Model predictive control (MPC) has received much attention in the control community [19] due to its ability to control multi-input and multi-output systems while handling constraints. An MPC is a real-time optimization method, where an optimization problem is solved online using a dynamic system model. A sequence of control actions is chosen over a specified horizon window to give the optimal control trajectory. However, from the computed control action sequence, only the first sample is implemented on the system. The model is then updated using the newly available information, and the control problem is solved again. This procedure is repeated continuously, and thus, it can update its control trajectory whenever new information becomes available.

A generalized formulation of the MPC optimization problem for a prediction horizon of  $N$  samples can be given by

$$\min_{u(k)} \sum_{k=1}^N J(x(k), u(k), d(k)) \quad (1)$$

$$\text{s.t. } x(k+1) = f(x(k), u(k), d(k)) \quad (2)$$

$$\underline{x}(k) \leq x(k) \leq \bar{x}(k) \quad (3)$$

$$\underline{u}(k) \leq u(k) \leq \bar{u}(k). \quad (4)$$

The control objective is defined by  $J(\cdot)$ , and  $f(\cdot)$  is the dynamic model of the system. The states, control inputs, and disturbances are represented with  $x$ ,  $u$ , and  $d$ , respectively. The maximum and minimum constraints for the states and control inputs are given by  $\{\underline{x}, \bar{x}\}$ , and  $\{\underline{u}, \bar{u}\}$ .

Traditionally, linear system models and linear constraints with a quadratic objective function are used, but implementation with nonlinear models, i.e., nonlinear MPC, is becoming more popular [19, 20]. However, in this work, only a linear MPC will be considered to simplify the computational complexity. In either case, the MPC algorithm's success will heavily depend on the accuracy of its model.

### B. Battery model and charging constraints

The state of charge (SoC) dynamics for an EV battery can be modeled using the discrete-time state equation [21]:

$$SoC_l(k+1) = SoC_l(k) + \frac{\eta_l P_{EV,l}(k) \Delta t}{E_l^{cap}}. \quad (5)$$

Here,  $\eta_l$  is the charging efficiency coefficient, and  $E_l^{cap}$  is the energy capacity for the charging EV's battery. The power absorbed by the battery is given by  $P_{EV,l}$ , and  $\Delta t$  is the sampling time. The subscripts  $l$  indicate the  $l$ :th charger in the FCS. The value of  $\eta_l$  will vary, depending on whether the battery is being charged or discharged. However, for this application, the EVs will not be allowed to provide V2G services that inject active power to the grid. Thus, it will be assumed that only charging the EVs is possible at the FCS.

The maximum charging rate for an EV will depend on the EV model and its battery. Some examples of EVs, their battery size, and their maximum charging rate are listed in Table I. However, the EVs will not always be allowed to charge at

TABLE I  
EV MODELS WITH BATTERY SIZE AND MAX. CHARGING POWER

EV Model	Battery Size	Max. charging rate
Audi e-tron	95 kWh	155 kW
Mercedes EQC	80 kWh	115 kW
Tesla S/X LR	90 kWh	140 kW
Nissan Leaf	30 kWh	45 kW

their maximum power since it would be harmful to the battery. Instead, the allowed power input to the battery is determined by the battery management system (BMS) and depends on different factors such as SoC and temperature. Here, it will be assumed that the allowed charging rate is only dependent on the SoC to reduce the complexity. The Dutch company Fastned [22], has tested different EVs on their chargers and collected the data to develop power curves as a function of SoC. These are nonlinear curves but have here been simplified to consist of piecewise linear functions, as illustrated in Fig. 1.

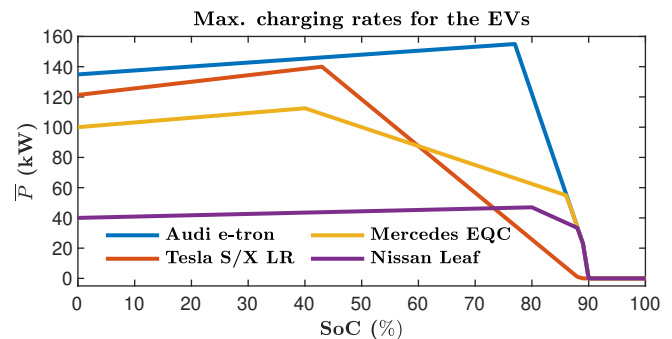


Fig. 1. Maximum charging rate curves for the EV batteries.

Based on the power curves in Fig. 1, the maximum power constraint for the EVs can be given by the linear function:

$$\bar{P}_{EV,l}(k) := a_l \cdot SoC_l(k) + b_l, \quad (6)$$

where  $a_l$  and  $b_l$  are constants that are determined based on the EV model at the  $l$ :th charger and its current SoC. In case no EV is connected to a charger, then the maximum power constraint will be set to zero. The minimum active power constraint for the charging EVs will always be zero to ensure that they can only be charged at the FCS.

### C. Grid voltage model and constraints

The power flow equations for the active and reactive power flows in a power network are given by [23]:

$$P_i = U_i \sum_{j=i}^{N_{bus}} Y_{ij} U_j \cos \delta_{ij} \quad (7)$$

$$Q_i = U_i \sum_{j=i}^{N_{bus}} Y_{ij} U_j \sin \delta_{ij}, \quad (8)$$

where  $U_i$  is the voltage amplitude in node  $i$  with  $Y_{ij}$ , and  $\delta_{ij}$  being the admittance and power angle between node  $i$  and  $j$ , respectively. The power flow equations are nonlinear and can be challenging to solve. To reduce the computational burden and assuming that the deviations from the nominal values are small, the power flow equations in (7) and (8) can be linearized around the current operating point. The resulting Jacobian matrix  $\mathcal{J}$  is then inverted to give an expression, describing the influence of  $\Delta P$  and  $\Delta Q$  on  $\Delta U$  and  $\Delta \delta$ :

$$\begin{bmatrix} \Delta U \\ \Delta \delta \end{bmatrix} = \mathcal{J}^{-1} \begin{bmatrix} \Delta P \\ \Delta Q \end{bmatrix}, \text{ where } \mathcal{J} := \begin{bmatrix} \frac{dP}{\partial U} & \frac{dP}{\partial \delta} \\ \frac{dQ}{\partial U} & \frac{dQ}{\partial \delta} \end{bmatrix}. \quad (9)$$

Here,  $\Delta P$ ,  $\Delta Q$ ,  $\Delta U$ , and  $\Delta \delta$  are the changes in active power, reactive power, voltage amplitudes and power angles, respectively. A discrete-time state-space model for the network bus voltages and power angles is then be given by

$$\begin{bmatrix} U(k+1) \\ \delta(k+1) \end{bmatrix} = \begin{bmatrix} U(k) \\ \delta(k) \end{bmatrix} + \mathcal{J}^{-1} \begin{bmatrix} \Delta P(k) \\ \Delta Q(k) \end{bmatrix}. \quad (10)$$

In which  $U(k)$  and  $\delta(k)$  are vectors containing the voltage magnitudes and voltage angles for the different buses in the distribution network at time  $k$ .

The Jacobian matrix in (9) can be updated at every iteration after new measurements become available. This will improve the model accuracy and result in more suitable values for  $\Delta P(k)$  and  $\Delta Q(k)$  to ensure that the voltage stays within the allowed limits:

$$\underline{U} \leq U(k) \leq \bar{U}. \quad (11)$$

### D. Grid feeding converter

A grid-feeding converter is primarily designed to draw or deliver a specified amount of power from or to the grid. The converter should be able to stay synchronized to the voltage and frequency at the connection point [24]. It operates by trying to produce or absorb a set amount of active  $P$  and reactive power  $Q$  through some set-points. Using  $\Delta P$  and  $\Delta Q$  as the manipulated variables for the MPC, the resulting set-point trajectories given to the converter are:

$$P(k+1) = P(k) + \Delta P(k) \quad (12)$$

$$Q(k+1) = Q(k) + \Delta Q(k). \quad (13)$$

The maximum amount of active and reactive power that can be generated will be determined by the specifications of the

converter. In this paper, the upper limit is assumed to only be given by the maximum apparent power such that:

$$P^2 + Q^2 \leq \bar{S}^2. \quad (14)$$

However, in addition to (14), the limit on the active power supplied to an EV is also restricted by the constraint in (6).

### E. MPC objective function

The profitability of an FCS will be determined by the amount of energy (kWh) it can sell. Thus, for the time EVs are connected to the chargers, the goal should be to maximize the supplied active power. An objective function with a time horizon of  $N$  and  $n$  number of chargers can be defined as:

$$\Phi := \sum_{k=1}^N \sum_{l=1}^n w_1 \left( P_{ref,l} - P_{EV,l}(k) \right)^2 + w_2 Q_{EV,l}^2(k). \quad (15)$$

Here,  $P_{EV,l}$ , and  $Q_{EV,l}$  are the set-points for the active power and reactive power to the  $l$ :th charger, respectively. The reference  $P_{ref,l}$ , is a value that is given by

$$P_{ref,l} = \begin{cases} P^{max} & \text{if an EV is connected to charger } l, \\ 0 & \text{otherwise,} \end{cases} \quad (16)$$

where,  $P^{max}$  is the maximum power capacity of the converter, which differs from the maximum power constraint for the EVs in (6). The weights  $w_1$  and  $w_2$  are scalar values and should be chosen such that  $w_1, w_2 > 0$ . Typically, these should be selected such that  $w_1 \gg w_2$ , since the last term in (15) is only there to ensure that reactive power is not injected to the grid unless it is necessary.

### F. MPC formulation for the FCS

Using the objective function in (15); the models for the batteries, the bus voltages, the power trajectories in (5), (10), (12), and (13), respectively; together with the constraints in (11) and (6), the MPC formulation can be given by:

$$\min_{\substack{\Delta P_{EV_1}, \dots, \Delta P_{EV_n}, \\ \Delta Q_{EV_1}, \dots, \Delta Q_{EV_n}}} \Phi + w_3 \epsilon^2 \quad (17)$$

$$\text{s.t. } U(k+1) = U(k) + \mathcal{J}_{\{U, EV\}}^{-1} \begin{bmatrix} \sum_l^n \Delta P_{EV,l} \\ \sum_l^n \Delta Q_{EV,l} \end{bmatrix}, \quad (18)$$

$$\underline{U}(k) - \epsilon \leq U(k) \leq \bar{U}(k) + \epsilon, \quad (19)$$

$$SoC_l(k+1) = SoC_l(k) + \eta_l P_{EV,l}(k) \Delta t / E_l^{cap}, \quad \forall l, \quad (20)$$

$$P_{EV,l}(k+1) = P_{EV,l}(k) + \Delta P_{EV,l}(k), \quad \forall l, \quad (21)$$

$$Q_{EV,l}(k+1) = Q_{EV,l}(k) + \Delta Q_{EV,l}(k), \quad \forall l, \quad (22)$$

$$0 \leq P_{EV,l}(k) \leq a_l \cdot SoC_l(k) + b_l, \quad \forall l, \quad (23)$$

$$\bar{S}^2 \geq P_{EV,l}^2(k) + Q_{EV,l}^2(k), \quad \forall l. \quad (24)$$

In (18), the power angles have been excluded from (10) since only the voltage magnitudes are considered. In addition, only  $\Delta P_{EV,l}$  and  $\Delta Q_{EV,l}$  for the different chargers can be controlled by the MPC. Therefore,  $\mathcal{J}^{-1}$  has been replaced with  $\mathcal{J}_{\{U, EV\}}^{-1}$ , where the subscript " $\{U, EV\}$ " represents the rows and columns in  $\mathcal{J}^{-1}$  that maps  $\sum_l^n \Delta P_{EV,l}$  and  $\sum_l^n \Delta Q_{EV,l}$  to  $\Delta U$ .

The term  $\epsilon$  has been added to the objective function and the voltage constraints to avoid the solution becoming infeasible. By selecting the weights such that  $w_3 \gg w_2 \gg w_1 > 0$ , the optimal solution for the above MPC problem will distribute the active power equally between the charging EVs while ensuring that the voltage at every bus stays within the allowed limits. When the voltage goes outside of the allowed threshold, the MPC will prioritize injecting the grid with reactive power to avoid having to reduce the active power that is being absorbed by the charging EVs. Even though the MPC objective tries to charge each EV at the converter's maximum power capacity, the upper limit between the EVs varies depending on the type and the current SoC. Therefore, the amount of reactive power available at each charger varies over time due to the constraint in (24). The MPC will try to take advantage of this by coordinating the reactive power between the converters to avoid needing to reduce the charging rates for the EVs.

### III. RESULTS AND DISCUSSION

The proposed MPC scheme was simulated using a model of an MV distribution grid. The MPC was implemented in Matlab using YALMIP [25], with a sampling time of 1 minute and a time horizon of 10 minutes. To solve the convex but quadratically constrained optimization problem, the solver SDPT3 was used [26].

#### A. The distribution grid model

The grid model used is based on a real MV radial distribution grid that is located in the municipality of Stange in Norway. The topology of the distribution system is shown

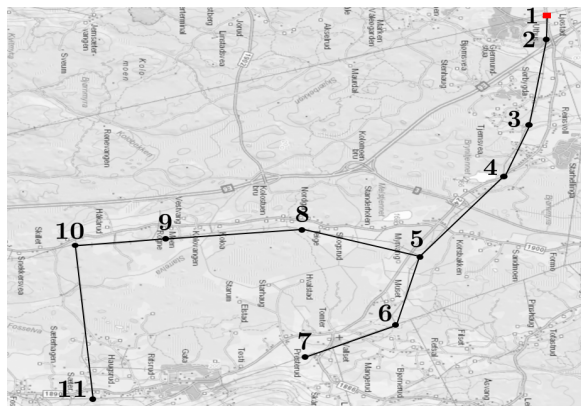


Fig. 2. Topology of the Stange distribution grid, adapted from [27].

in Fig. 2, where the grid is connected to a 66 kV / 22 kV substation at bus 1. There are 11 different buses, where 7 of them are connected to some time-varying load. The different loads consist primarily of different households and farms, but bus 11 is also connected to some schools and a grocery shop. The load profiles for a given day are shown in Fig. 3, but for more information about the Stange distribution grid, the cross-section for its lines, and admittances, the reader is referred to [27]. The voltage at bus 1 will remain constant at a value of 1 p.u., which is sufficient to keep the voltages at every bus within  $\pm 5\%$  under normal operation for the loads in Fig. 3.

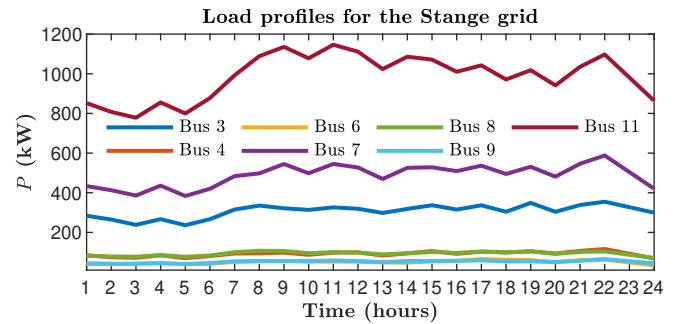


Fig. 3. Load profiles for the Stange distribution grid.

#### B. FCS and arriving EVs

The FCS is placed at bus 10 and consists of 10 separate chargers, each capable of delivering a maximum output of 150 kW. The number of EVs that are assumed to be visiting the FCS at every given hour for a given day is shown in Fig. 4. In

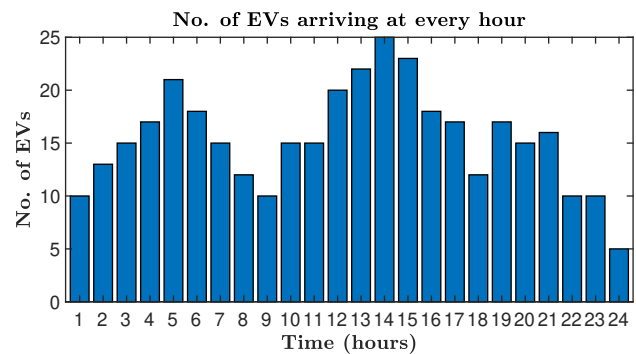


Fig. 4. The total number of EVs that arrive to the FCS at every hour.

[8], a Poisson process was used to estimate the arrival time for each EV based on the number of EVs expected to arrive per minute, for a given hour. However, in this paper, the arrival times for the EVs are simply distributed evenly for the given number of EVs at every hour.

According to its arrival time, each EV will arrive at the FCS and occupy the first available charger to start charging. When multiple EVs want to charge simultaneously, a queue will start to form since there will not always be chargers that are immediately available. Consequently, the queuing EVs will be forced to wait until a charging spot becomes available. For these simulations, the maximum waiting time for the EVs has been set to 15 minutes, i.e., an EV will leave the queue after 15 minutes, and the FCS will lose a customer.

The EV fleet is represented by the different EV models, listed in Table I, which influence the battery size, and the charging rate based on the power curve in Fig. 1. The EV models and the initial SoC are randomly assigned to the EV fleet, with the initial SoC being within 15 and 35%. However, the same data set of the EV types and their initial SoC will be used for all simulations. Once an EV is being charged, it will leave the FCS when it reaches an SoC of 90%, or the duration it has been occupying the charger exceeds 1 hour.

### C. FCS Controller

The FCS controller's objective is to coordinate and control the different chargers such that the maximum energy can be supplied to the charging EVs without the voltages dropping below the allowed limit. By maximizing the active power output, the EVs can be charged faster, and thus, more charging slots can become available. As a result, more EVs can charge, which increases the profitability of the FCS.

To demonstrate the benefits of using an MPC and optimally utilizing the available reactive power, the FCS is controlled using four different methods. First, the FCS is controlled at its maximum capacity, while ignoring its impact on the voltage. In the second case, a constant upper limit on the total active power is placed on the FCS to ensure the voltage does not drop under its threshold. In the third and fourth methods, an MPC is used to keep the voltage within the allowed limits by continuously adjusting the power output. Therefore, the lower and upper limits in (19) has been set to 0.95 and 1.05 p.u, respectively. However, in case 3, only the active power  $P$  is adjusted, keeping the reactive power  $Q$  at zero, whereas in case 4, both active and reactive power are controlled.

1) *Case 1: FCS operating at maximum capacity:* In this case, the EVs are always charged at their maximum charging rates, without considering the grid voltages. For the FCS operator, this is the most profitable method of controlling the chargers, but it has a very negative impact on the grid voltage, as can be seen in Fig. 5. The voltage at bus 11 is the most critical and will, thus, only be displayed here. When operating the FCS at its maximum capacity, it will deliver the most energy and hence charge the highest number of EVs, but the voltage will also fall below its limit for most of the day.

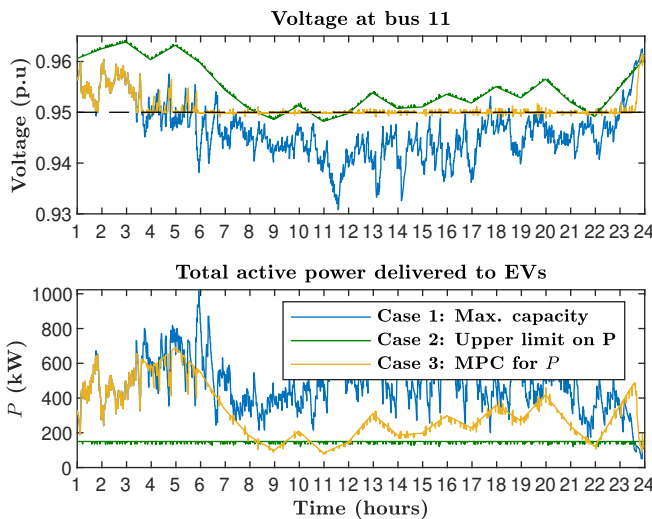


Fig. 5. Voltage at bus 11 and delivered power to EVs for case 1, 2, and 3.

2) *Case 2: Constant limit on the active power:* Typically, an upper limit on the power demand is placed by the grid operator on the FCS to ensure that, e.g., the voltage never drops below its lower limit. A 150 kW upper limit was used in this example, which must be shared between all the ten

chargers. The simulation results from placing this constraint on the FCS are available in Fig. 5, which shows that the voltage remains above the limit for most of the simulation. However, in this case, the FCS only manages to charge 240 EVs out of 371 and deliver a total of 3.54 MWh, as shown in Table II, which constitutes only 31 % of the FCS's capacity.

TABLE II  
ENERGY DELIVERED TO EVs AND NO. OF EVs CHARGED

Control method	Delivered energy	No. of EVs charged
Maximum capacity	11.29 MWh	356 / 371
Upper limit on $P$	3.54 MWh	240 / 371
MPC controlling $P$	7.24 MWh	280 / 371
MPC controlling $P$ & $Q$	11.23 MWh	351 / 371

3) *Case 3: MPC for active power control:* Placing an upper limit on the total active power can ensure that grid voltages stay within allowable limits. However, according to Fig. 5, it can be seen that for case 2, the voltage drop is primarily an issue around the 9:th, 11:th, and 22:th hour. Therefore, instead of having a constant upper restriction on  $P$ , an MPC can continuously adjust the active power to avoid the voltage dropping below the threshold. The results are shown in Fig. 5 and Table II, and shows a significant improvement compared to the second case. A total of 7.24 MWh can be delivered to the EVs, which is 64 % of what is possible without the voltage at bus 11 going below 0.95 p.u.

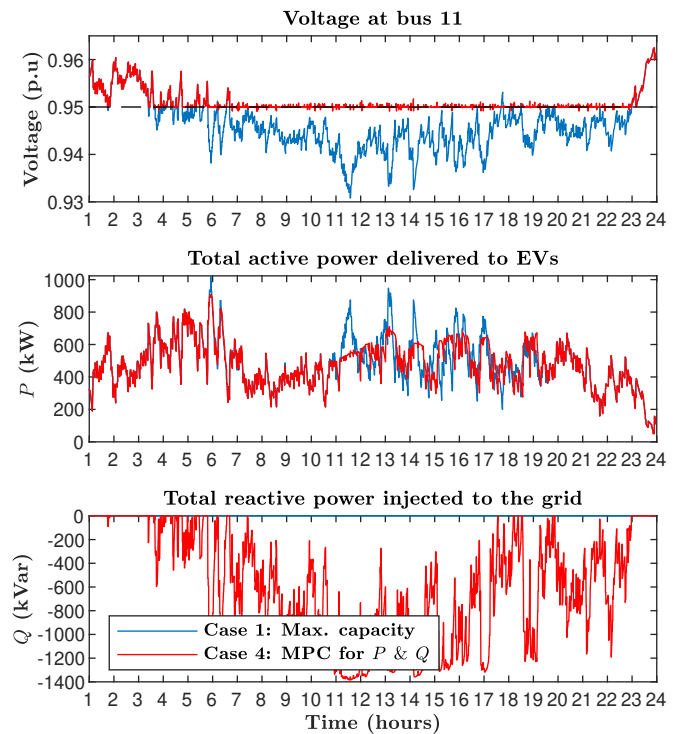


Fig. 6. Voltage at bus 11, the delivered power to EVs and the reactive power injected to the grid for case 1, and 4.

#### 4) Case 4: MPC for active and reactive power control:

In the previous cases, only active power was used, and thus, the reactive power remained an unused resource. The reactive power is limited by the constraint in (24), which is set to 150 kVA for each charger. Therefore, the availability of  $Q$  will be dependent on  $P$ . However, the maximum charging rate varies depending on the SoC and EV type, and thus, there will almost always be some reactive power available without needing to reduce  $P$ . Using the proposed MPC formulation, the optimal references for  $P$  and  $Q$  will continuously be sent to the individual chargers. The simulation results are shown in Fig. 6 and are compared to case 1. The total amount of energy delivered to the EVs when using the proposed MPC is almost identical (99 %) to charging every EVs at their maximum charging rate. However, by taking advantage of the chargers' reactive power, the voltage can be kept above 0.95 p.u.

#### IV. CONCLUSION AND FURTHER WORK

High-power charging of EVs can cause power quality issues such as voltage drops, and therefore, it is common to restrict FCS in terms of their maximum active power drawn from the grid. An MPC was used to control and coordinate chargers in an FCS to maximize the delivered active power to the EVs while simultaneously supporting the grid by injecting reactive power. It was demonstrated through simulations that the active power used for charging could significantly be increased while ensuring that the grid voltages stayed within acceptable limits when the reactive power was utilized in a near-optimal way. Therefore, even though reactive power, as for today, has no direct economic value, it can provide an indirect economic benefit by controlling the voltage. Instead of limiting the maximum active power drawn from the grid, the grid operators could, e.g., set restrictions on the voltages, which would provide more flexibility and opportunities for FCS operators to take advantage of already existing resources. Future research will investigate the use of chargers for other ancillary services and the feasibility of bi-directional converters. Additional work will also involve developing simpler control structures that are easier to implement but can still give comparable results.

#### ACKNOWLEDGMENT

The authors gratefully acknowledge the FuChar project consortium for contributing to this work with their knowledge and experience. We are also grateful to Jon Are Suul and Giuseppe Guidi for valuable discussions and input regarding state-of-the-art converter and charging technology.

#### REFERENCES

- [1] H. Khalkhali and S. H. Hosseini, "Multi-stage stochastic framework for simultaneous energy management of slow and fast charge electric vehicles in a restructured smart parking lot," *International Journal of Electrical Power and Energy Systems*, vol. 116, 2020.
- [2] M. Neaimeh, S. D. Salisbury, G. A. Hill, P. T. Blythe, D. R. Scofield, and J. E. Francfort, "Analysing the usage and evidencing the importance of fast chargers for the adoption of battery electric vehicles," *Energy Policy*, vol. 108, pp. 474–486, 2017.
- [3] K. Clement-Nyns, E. Haesen, and J. Driesen, "The impact of Charging plug-in hybrid electric vehicles on a residential distribution grid," *IEEE Transactions on Power Systems*, vol. 25, no. 1, pp. 371–380, 2010.
- [4] J. A. Lopes, F. J. Soares, and P. M. Almeida, "Integration of electric vehicles in the electric power system," *Proceedings of the IEEE*, vol. 99, no. 1, pp. 168–183, 2011.
- [5] A. Di Giorgio, F. Liberati, and S. Canale, "Electric vehicles charging control in a smart grid: A model predictive control approach," *Control Engineering Practice*, vol. 22, no. 1, pp. 147–162, 2014.
- [6] H. Vincent Poor, Y. Shi, H. D. Tuan, A. V. Savkin, and T. Q. Duong, "Model predictive control for smart grids with multiple electric-vehicle charging stations," *IEEE Transactions on Smart Grid*, vol. 10, no. 2, pp. 2127–2136, 2019.
- [7] Ionity, "Technology." [Online]. Available: <https://ionity.eu/en/design-and-tech.html>, [accessed 10- Oct- 2020].
- [8] E. Ivarøy, B. N. Torsæter, and M. Korpås, "Stochastic Load Modeling of High-Power Electric Vehicle Charging - A Norwegian Case Study," in *2020 International Conference on Smart Energy Systems and Technologies (SEST)*, 2020.
- [9] H. Tan, D. Chen, and Z. Jing, "Optimal Sizing of Energy Storage System at Fast Charging Stations under Electricity Market Environment," *IEEE 2nd Int. Conference on Power and Energy Applications*, pp. 7–10, 2019.
- [10] S. Habib, M. Kamran, and U. Rashid, "Impact analysis of vehicle-to-grid technology and charging strategies of electric vehicles on distribution networks - A review," *Journal of Power Sources*, vol. 277, pp. 205–214, 2015.
- [11] T. U. Solanke, V. K. Ramachandaramurthy, J. Y. Yong, J. Pasupuleti, P. Kasinathan, and A. Rajagopalan, "A review of strategic charging–discharging control of grid-connected electric vehicles," *Journal of Energy Storage*, vol. 28, 2020.
- [12] K. Uddin, M. Dubarry, and M. B. Glick, "The viability of vehicle-to-grid operations from a battery technology and policy perspective," *Energy Policy*, vol. 113, pp. 342–347, 2018.
- [13] G. Saldaña, J. I. S. Martin, I. Zamora, F. J. Asensio, and O. Oñederra, "Electric vehicle into the grid: Charging methodologies aimed at providing ancillary services considering battery degradation," *Energies*, vol. 12, no. 12, 2019.
- [14] A. Thingvad, C. Ziras, and M. Marinelli, "Economic Value of Electric Vehicle Reserve Provision in the Nordic Countries under Driving Requirements and Charger Losses," *Journal of Energy Storage*, vol. 21, pp. 826–834, 2019.
- [15] V. Monteiro *et al.*, "Assessment of a battery charger for Electric Vehicles with reactive power control," in *IECON 2012*, pp. 5142–5147, 2012.
- [16] C. H. Dharmakeerthi, N. Mithulanathan, and T. K. Saha, "Impact of electric vehicle fast charging on power system voltage stability," *International Journal of Electrical Power and Energy Systems*, vol. 57, pp. 241–249, 2014.
- [17] P. Włodarczyk, A. Sumper, and M. Cruz, "Voltage control of distribution grids with multi-microgrids using reactive power management," *AECE*, vol. 15, no. 1, pp. 83–88, 2015.
- [18] S. Paudyal, O. Ceylan, B. P. Bhattarai, and K. S. Myers, "Optimal coordinated EV charging with reactive power support in constrained distribution grids," in *Power & Energy Society General Meeting*, 2017.
- [19] S. J. Qin and T. A. Badgwell, "A survey of industrial model predictive control technology," *Control Engineering Practice*, vol. 11, no. 7, pp. 733–764, 2003.
- [20] F. Allgöwer, R. Findeisen, and Z. K. Nagy, "Nonlinear Model Predictive Control: From Theory to Application," *Tech. Rep.* 3, 2004.
- [21] M. Legry, F. Colas, C. Saudemont, J. Y. Dieulot, and O. Ducarme, "A two-layer model predictive control based secondary control with economic performance tracking for islanded microgrids," in *IECON 2018*, pp. 77–82, 2018.
- [22] Fastned, "Fastned charging curve." [Online]. Available: <https://support.fastned.nl/hc/en-gb>, [accessed 5- Aug- 2020].
- [23] Prabha Kun, ed., *Power System Stability and Control*. New York: New York: McGraw, 1994.
- [24] A. M. Bouzid, J. M. Guerrero, A. Cheriti, M. Bouhamida, P. Sicard, and M. Benghanem, "A survey on control of electric power distributed generation systems for microgrid applications," *Renewable and Sustainable Energy Reviews*, vol. 44, pp. 751–766, 2015.
- [25] J. Löfberg, "YALMIP : A Toolbox for Modeling and Optimization in MATLAB," in *Proc. of the CACSD Conference*, (Taipei, Taiwan), 2004.
- [26] R. H. Tütüncü, K. C. Toh, and M. J. Todd, "Solving semidefinite-quadratic-linear programs using SDPT3," *Mathematical Programming, Series B*, vol. 95, no. 2, pp. 189–217, 2003.
- [27] E. Ivarøy, "Optimal planning of fast charging stations for EVs – A Norwegian case study," Master's thesis, NTNU, 2020.